Materials Science-Poland, Vol. 23, No. 2, 2005

Influence of the dislocation structure on the crack tip in highly deformed iron

K. BORYSOVSKA[1], V. SLYUNYAYEV[1], YU. PODREZOV[1*], Z. PAKIELA[2], K. KURZYDŁOWSKI[2]

[1] Institute for Problems of Materials Science, 3 Krzhizhanovsky, Kiev 03142, Ukraine

[2] Warsaw University of Technology, Faculty of Materials Science and Engineering, Wołoska 141, 02-507 Warsaw, Poland

Plastic deformation can produce materials with different structural states. Strained BCC-metals have been shown to undergo internal structural developments during plastic deformation. The interaction between quasi-cleavage crack and substructure was studied. The details of the influence of substructure on stress near the crack tip, structure rebuilding near the crack tip and the energy of dislocation movement were analyzed. The essential influence of the deformation substructure on the force and energy parameters of fracture processes was established.

Key words: *structural sensitivity; deformation structure; edge dislocation*

1. Introduction

Both strain hardening and fracture toughness reveal structural sensitivity depending on the interaction of a crack with the dislocation substructure. The hardening curve of each structural state can be approximated by straight lines in σ–$e^{0.5}$ true stress, e – true deformation coordinates as shown in Fig. 1. The structural sensitivity of fracture toughness was analyzed in the previous paper [1] as shown in Fig. 2. The main task of modelling is to analyze the interaction of a crack tip and an edge dislocation in the plastic zone with a dislocation substructure (forest of dislocations, cell walls and boundary of nanograin).

The assumption made for model proposed are:

- Fracture mechanism is quasi-cleavage.
- The size of the plastic site created by a dislocation source near the crack tip is not less than the grain size.

* Corresponding author, e-mail: podrezov@materials.kiev.ua

• The external stress is constant, and the evolution of the structure occurs in the real time.

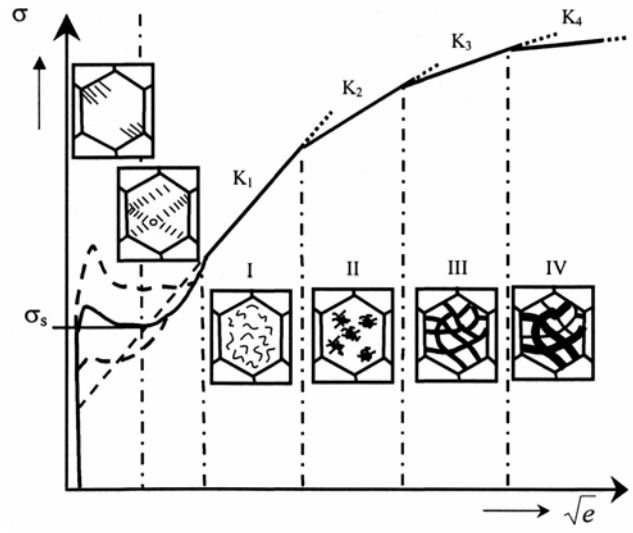

Fig. 1. Deformation hardening curve in σ–$e^{0.5}$ coordinates: I – single dislocations, II – dislocation loops and pile-up, III – low angle cells; IV – high angle cells

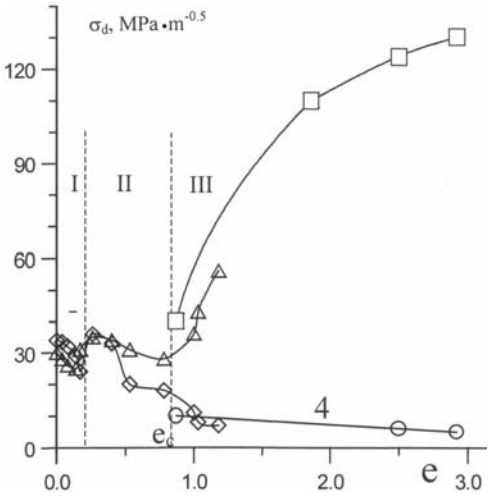

Fig. 2. Fracture toughness of strained iron vs. deformation degree [1]: △, ◇ – rolling, ✳, ○ – ECAP (△, ✳ – crack introduced into the plane perpendicular to the plane of deformation; ◇, ○ – crack introduced into the plane parallel to the plane of deformation); I – single dislocations and pile-up; II – low angle cell structure; III – high angle cell structure

The stress effects on the dislocation near the crack tip are calculated in accordance with Ohr's model [2], and are shown in Fig. 3.

The total stress is obtained by adding the crack stress, which is repulsive, and the image stress which is attractive. The crack stress components are:

$$\begin{cases} \sigma_{22} = \sigma\sqrt{\dfrac{a}{2r}}\cos\dfrac{\Theta}{2}\left(1+\sin\dfrac{\Theta}{2}\sin\dfrac{3\Theta}{2}\right) \\ \sigma_{11} = \sigma\sqrt{\dfrac{a}{2r}}\cos\dfrac{\Theta}{2}\left(1-\sin\dfrac{\Theta}{2}\sin\dfrac{3\Theta}{2}\right) \\ \sigma_{12} = \sigma\sqrt{\dfrac{a}{2r}}\sin\dfrac{\Theta}{2}\cos\dfrac{\Theta}{2}\cos\dfrac{3\Theta}{2} \end{cases}$$

where a – length of the crack, r – distance between dislocation and crack tip, Θ – angle between x-axis and the line which connects the crack tip.

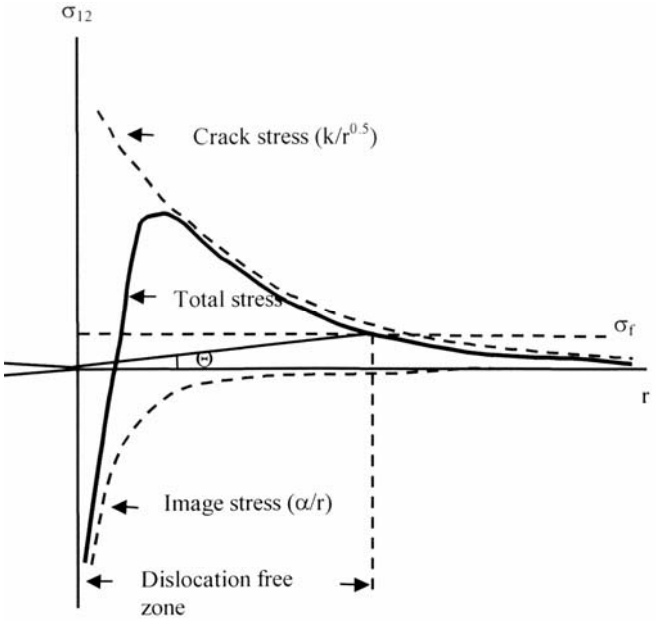

Fig. 3. Stress effects on the dislocation near crack tip [2]

The dislocation can glide if the stress is greater than the friction stress σ_f. In the case, when more than one dislocation remains near the crack tip, the total stress consists of the crack stress, the self-image stress, the image stress from other dislocations [4–6]. The stress component on an edge dislocation 2 (x, y) from edge dislocation 1 can be found from the following expression (Fig. 4):

$$\sigma_{12} = -\sigma_{11}\cos\beta\sin\beta + \sigma_{22}\sin\beta\cos\beta + \sigma_{12}(\cos^2\beta - \sin^2\beta)$$

$$\sigma_{11} = \sigma_{11}\cos^2\beta + \sigma_{22}\sin^2\beta + 2\sigma_{12}\cos\beta\sin\beta$$

$$\sigma_{22} = \sigma_{11}\sin^2\beta + \sigma_{22}\cos^2\beta - 2\sigma_{12}\cos\beta\sin\beta$$

where

$$\sigma_{11} = \frac{Gb}{2\pi(1-\nu)} \frac{y(3x^2 + y^2)}{(x^2 + y^2)^2}$$

$$\sigma_{22} = \frac{Gb}{2\pi(1-\nu)} \frac{y(x^2 - y^2)}{(x^2 + y^2)^2}$$

$$\sigma_{11} = \frac{Gb}{2\pi(1-\nu)} \frac{x(x^2 - y^2)}{(x^2 + y^2)^2}$$

and b is the Burgers vector, G – shear module, β – angle between x and line, which connects dislocation 1 and dislocation 2.

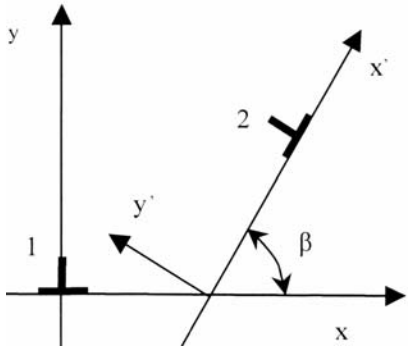

Fig. 4. Edge dislocations located in parallel slip planes

The interaction of a cleavage crack and dislocations emitted from the crack tip with the deformation substructure was calculated. In this paper the following cases of substructures are considered: no wall; chaotic distribution of dislocation; a moving dislocation wall; a non-moving penetrable by a lattice dislocation; and a substructure not penetrable by a lattice dislocation.

The calculated algorithm was achieved as follows:

1 step: to calculate total stress on all moving dislocations at the time t and at a given internal stress (100 MPa.).

2 step: to calculate the speed of each moving dislocation.

3 step: to calculate the new position of each moving dislocation.

4 step: to calculate the stress (σ_{22}) from all the dislocations at the distance $2b$ from the crack tip (σ_d).

5 step: to calculate the movement energy (E) (the increase of movement energy is $\sigma bvdt$) of all moving dislocations (v – rate of dislocation, dt – time step).

6 step: to calculate the stress on the source located at the distance $2b$ from crack tip; if this stress is higher than the yield stress then two dislocations are emitted.

7 step: $t = t + dt$ ($dt = 3\times10^{-13}$ sec) $\Rightarrow$ 1 step.

In this work, the dislocation wall consists of 100 dislocations at the distance 100b from the crack tip and has a length of 500b. The parameters of the material (iron) are: Shear modules G = 84 GPa, Burger vector $b = 2.8\times10^{-10}$ m, Poisson ratio $\nu = 0.29$, yield stress σ_{yi} =100 MPa.

2. Results

The results of our calculation are shown in Figs. 5–9.

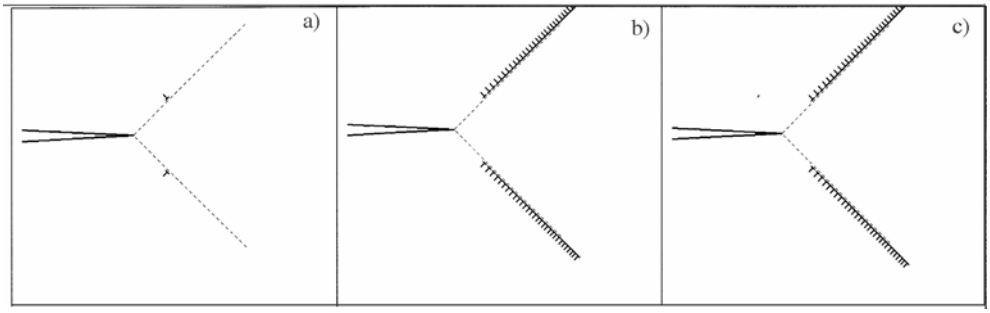

Fig. 5. Movement of dislocations emitted from crack tip in ironcrystal of iron without deformation substructure (case I): a) $t = 1\times10^{-13}$ sec, $E = 3\times10^{-6}$ J, $\sigma_d = -3\times10^{3}$ MPa, b) $t = 50\times10^{-13}$ sec, $E = 1.74\times10^{-4}$ J, $\sigma_d = -8.1\times10^{3}$ MPa, c) $t = 100\times10^{-13}$ sec, $E = 3.62\times10^{-4}$ J, $\sigma_d = -1.37\times10^{5}$ MPa

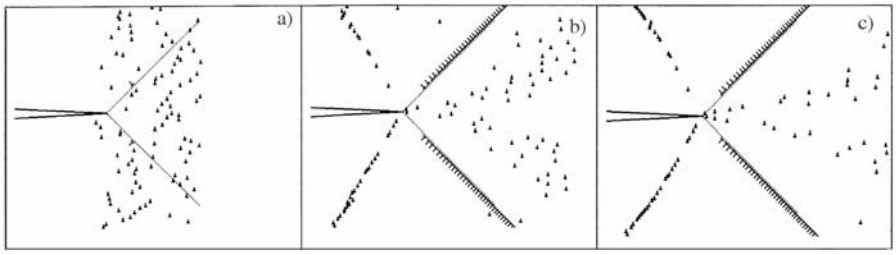

Fig 6. Movement of dislocation near crack tip on monocrystal of iron with chaotic distribution of dislocation (case II): a) $t = 1\times10^{-13}$ sec, $E = 3\times10^{-6}$ J, $\sigma_d = -3\times10^{3}$ MPa, b) $t = 50\times10^{-13}$ sec, $E = 1.60\times10^{-4}$ J, $\sigma_d = -9.1\times10^{4}$ MPa, c) $t = 100\times10^{-13}$ sec, $E = 3.18\times10^{-4}$ J, $\sigma_d = -1.47\times10^{5}$ MPa

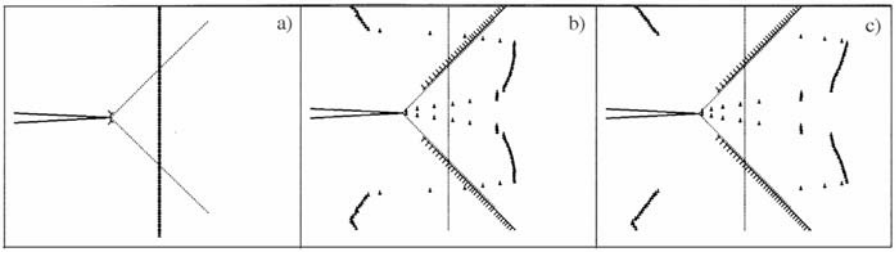

Fig. 7. Movement of dislocation near crack tip in iron crystal with moving dislocation wall (case III): a) $t = 1\times10^{-13}$ sec, $E = 2.7\times10^{-6}$ J, $\sigma_d = -6\times10^{3}$ MPa, b) $t = 50\times10^{-13}$ sec, $E = 1.60\times10^{-4}$ J, $\sigma_d = -9.5\times10^{4}$ MPa, c) $t = 80\times10^{-13}$ sec, $E = 2.522\times10^{-4}$ J, $\sigma_d = -1.28\times10^{5}$ MPa

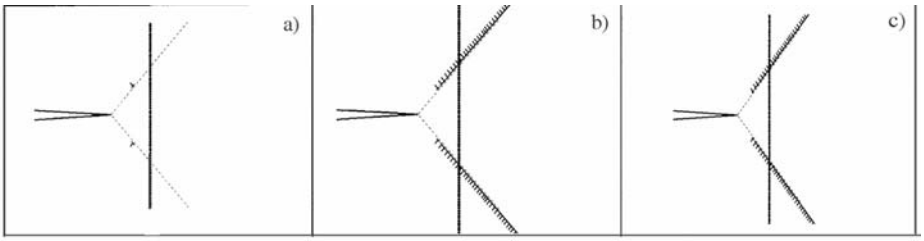

Fig. 8. Movement of dislocation emitted from crack tip in iron crystal with nonmoving wall, penetrable by dislocation (case IV): a) $t = 1\times10^{-13}$ sec, $E = 2\times10^{-6}$ J, $\sigma_d = -10\times10^{3}$ MPa, b) $t = 50\times10^{-13}$ sec, $E = 1.40\times10^{-4}$ J, $\sigma_d = -8.9\times10^{4}$ MPa, c) $t = 100\times10^{-13}$ sec, $E = 3.006\times10^{-4}$ J, $\sigma_d = -1.47\times10^{5}$ MPa

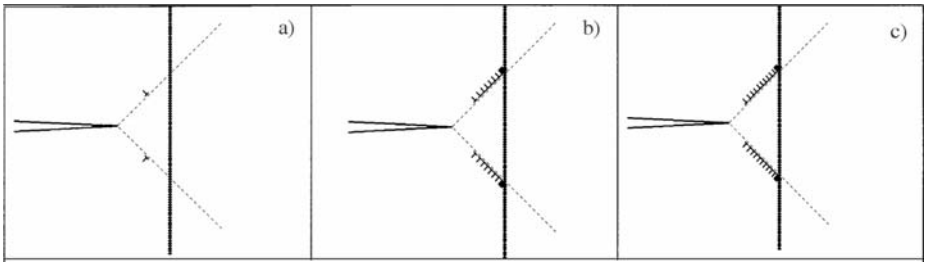

Fig. 9. Movement of dislocation emitted from crack tip in iron crystal with nonmoving wall, nonpenetrable for dislocation (case V): a) $t = 1\times10^{-13}$ sec, $E = 2\times10^{-6}$ J, $\sigma_d = -10\times10^{3}$ MPa, b) $t = 50\times10^{-13}$ sec, $E = 1.19\times10^{-4}$ J, $\sigma_d = -1.16\times10^{4}$ MPa, c) $t = 1\times10^{-11}$ sec, $E = 2.02\times10^{-4}$ J, $\sigma_d = -2.26\times10^{5}$ MPa

The dependence of movement energy on time is shown in Fig. 10.

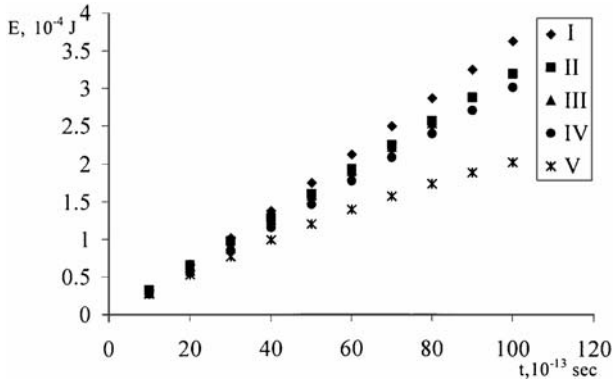

Fig. 10. The dependence of movement energy on time

The faster growth of energy is observed in case I (no substructure); in this case the substructure does not block the dislocation movement, which leads to energy growth. In case II (chaotic distribution) the substructural influence is weak, so energy growth in this case is higher than in case III (moving wall). Dislocations emitted from the crack tip mainly influence the energy in the selected parameters (high external stress), because it is located near the crack tip. Therefore, there is no essential difference be-

tween the energy in case III (movement wall) and case IV (non moving penetrable wall). In case V (non moving non penetrable wall) the energy is the lowest, because in this case the movement of dislocations is limited.

The dependence of σ_d (with inverse sign) on time is shown in Fig. 11.

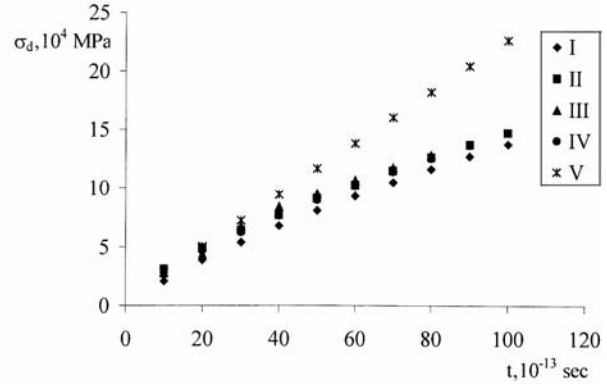

Fig. 11. The dependence of σ_d (with inverse sign) on time

The lower growth of σ_d is observed in case I (no substructure), in this case the substructure does not block the emitted dislocations and its movement away from the crack tip. There is no large difference between case II (chaotic distribution), case III (moving wall) and IV (nonmoving penetrable wall). Therefore, the wall cannot block the emitted dislocations at high external stress. In case V (nonmoving nonpenetrable wall) the σ_d growth is the faster, because in this case emitted dislocations are blocked and interact with the crack tip, causing blocking the emission of dislocation and suppression of crack development.

3. Conclusions

The interaction between a quasi cleavage crack and the substructure was studied. The details of the influence of substructure on the stress near crack tip, structure rebuilding near the crack tip and the energy of dislocation movement were analyzed. There is an essential influence of the deformation substructure on the force and energy parameters of the fracture processes. In this case the influence of a number of dislocations is lower than the influence of the substructure tip.

In case V (nonmoving nonpenetrable wall) the value of stress is essentially higher than in penetrable walls case, though the movement energy is lowest in this case. In cases II (chaotic distribution), III (moving wall) and IV (nonmoving penetrable wall) the difference between current movement energy or force parameter σ_d is not high, which is similar to the fracture toughness shown in Fig. 2.

References

[1] PODREZOV YU.N., DANILENKO N.I ., KOPYLOV V.I., FIRSTOV S.A, Phys. High Pressure, 11 (2001), 33.
[2] OHR S.M., Mater. Sci. Eng., 72 (1985), 1
[3] NOTT J., *Fundamentals of Fracture Mechanics*, Butterworths, London,1978.
[4] FERNEY B.D., HSIA K.J., Mater. Sci. Eng., A260 (1999), 1.
[5] HIRSCH P.B., ROBERTS S.G., SAMUELS J., Proc. R. Soc. London, A421 (1989), 25.
[6] BORYSOVSKA K.M., PODREZOV YU.M., SLYUNYAYEV V.M., Electron microscopy and material strength, (In Russian), (2002), 3

Received 9 September 2004
Revised 19 October 2004